



Contents lists available at ScienceDirect

Analytical Biochemistry

journal homepage: www.elsevier.com/locate/yabio

Quantitative measure of cytotoxicity of anticancer drugs and other agents

Zhimin Tao^a, Eyone Jones^a, Jerry Goodisman^{b,*}, Abdul-Kader Souid^a^a Department of Pediatrics, State University of New York, Upstate Medical University, Syracuse, NY 13210, USA^b Department of Chemistry, Syracuse University, Syracuse, NY 13244, USA

ARTICLE INFO

Article history:

Received 2 April 2008

Available online 18 June 2008

Keywords:

Cytotoxicity

Respiration

Phosphorescence

Oxygen consumption

ABSTRACT

Many anticancer drugs act on cancer cells to promote apoptosis, which includes impairment of cellular respiration (mitochondrial O₂ consumption). Other agents also inhibit cellular respiration, sometimes irreversibly. To investigate the sensitivity of cancer cells to cytotoxins, including anticancer drugs, we compare the profiles of cellular O₂ consumption in the absence and presence of these agents. Oxygen measurements are made at 37 °C, using glucose as a substrate, with [O₂] obtained from the phosphorescence decay rate of a palladium phosphor. The rate of respiration k is defined as $-d[O_2]/dt$ in a sealed container. Different toxins produce different profiles of impaired respiration, implying different mechanisms for the drug-induced mitochondrial dysfunction. The decrease in the average value of k over a fixed time period, I , is proposed as a characteristic value to assess mitochondrial injury. The value of I depends on the nature of the toxin, its concentration, and the exposure time as well as on the cell type. Results for several cell types and 10 cytotoxins are presented here.

© 2008 Elsevier Inc. All rights reserved.

Although the process of drug-induced tumor cell death remains poorly understood, many anticancer agents induce apoptosis through similar mechanisms such as the release of cytochrome *c* from mitochondria into cytosol and the consequent activation of caspases. The activated caspases then attack the permeabilized mitochondria, disrupt the mitochondrial electron transport chain, collapse the mitochondrial inner membrane potential, and diminish the mitochondrial structural integrity [1,2]. Interferences in the apoptotic scheme reduce cancer cells' sensitivity to therapy [3,4]. Because most anticancer drugs and other cytotoxic agents impair mitochondria directly or indirectly, their cytotoxicity can be easily assessed by measuring their effects on mitochondrial respiration. It is proposed here that measurement of cellular respiration in the presence and absence of an agent is a useful way to characterize cytotoxicity. In the case of an anticancer drug, this measurement becomes an index of the cell's sensitivity to treatment by the drug.

A variety of agents are studied here. The anthracycline antibiotic doxorubicin intercalates with DNA and produces DNA breaks by stimulating topoisomerase II cleavable complex formation [5]. In the cell, the quinone moiety of doxorubicin is reduced to the semiquinone radical, generating reactive oxygen species that directly damage cell organelles and induce apoptosis [6]. Dactinomycin is an important anticancer chromopeptide that intercalates between DNA base pairs and inhibits transcription [7]. Platinum (Pt)¹ com-

pounds, including cisplatin, carboplatin, oxaliplatin, and nedaplatin, bind to DNA and promote apoptosis [8]. The latter three Pt agents differ from cisplatin (the parent compound) in the different ligands occupying the Pt coordination spheres. These structural variations yield unique antitumor activity and toxicity profiles such as the reactivity with DNA and induction of apoptosis [8]. Transplatin, the geometric isomer of cisplatin, is expected to be less cytotoxic than cisplatin. Tirapazamine (3-amino-1,2,4-benzotriazine-1,4-dioxide) is a promising agent that is effective in hypoxic tumor environments [9]. The activated compound results from a two-electron reduction of tirapazamine, which is readily reoxidized to its parent form in aerobic conditions [10]. A highly cytotoxic hydroxyl radical (HO•) is released and produces DNA breaks, chromosomal aberrations, and eventually cell death [9–11]. Not considered as an anticancer drug, cyclosporine A (CsA) is an important immune suppressor. Its cellular targets include cyclophilin and calmodulin, modulating calcium fluxes through mitochondrial transition permeability (MTP) induced by Ca²⁺ accumulation in the cytosol [14,15]. In addition, it blocks Ca²⁺ efflux from mitochondria, causing calcium flood in the mitochondrial matrix that induces serious cytotoxicity and further injures mitochondrial respiration [16]. Finally, caffeine is known to activate Ca²⁺ channels on the plasma membrane and endoplasmic reticulum, rapidly accumulating Ca²⁺ in neighboring mitochondria, and this may impair their function. Caffeine also potentiates the cytotoxicity of anticancer drugs.

The purpose of this work is to define a characteristic cytotoxicity parameter that will be useful in pharmacology and toxicology. The parameter is the extent of inhibition of respiration, where inhibition is defined in terms of the ratio of the average rates of

* Corresponding author. Fax: +1 315 443 4070.

E-mail address: goodisma@mailbox.syr.edu (J. Goodisman).¹ Abbreviations used: Pt, platinum; tirapazamine, 3-amino-1,2,4-benzotriazine-1,4-dioxide; CsA, cyclosporine A; MTP, mitochondrial transition permeability; Pd, palladium; dH₂O, distilled water; EDTA, ethylenediaminetetraacetic acid.

respiration in the presence and absence of the cytotoxic agent. Both rates must be measured on cells from the same batch because rates depend on previous history and other uncontrollable factors. It is expected that the rate of respiration in the presence of the agent will depend on the agent's nature, its concentration, and the incubation time, as well as on the cell type, so that the inhibition will depend on all of these factors. For simplicity, the experiments discussed in this article are limited to two cell types: Jurkat and HL-60.

Respiration rate is obtained from the decrease in dissolved oxygen concentration in a closed vessel. Dissolved oxygen concentration is measured from the decay rate of phosphorescence from a palladium phosphor, present in the solution, using a homemade instrument [17–20]. In previous studies, we used this instrument to explore the mitochondrial perturbation during anticancer therapy in vitro as well as enzyme reactions involving O₂ [21–24]. The phosphorescence method of oxygen analysis has several advantages compared with electrochemical and other methods. It is totally noninvasive and does not affect the system being measured because no oxygen is consumed by the measurement. It allows measurement of [O₂] down to nanomolar concentrations. It can be used continuously for long periods of time with no deterioration (as for electrodes) or loss of accuracy, so that slow processes such as decrease in respiration rates can be followed. Furthermore, it requires only a single calibration, with no necessity to check the instrument during or after long runs.

Materials and methods

Reagents

Pd(II) complex of *meso*-tetra-(4-sulfonatophenyl)-tetra-benzoporphyrin (sodium salt, palladium [Pd] phosphor) was obtained from Porphyrin Products (Logan, UT, USA). Its solution (2.5 mg/ml = 2 mM) was prepared in distilled water (dH₂O) and stored at –20 °C in small aliquots.

Doxorubicin HCl (3.45 mM) was purchased from Bedford Laboratories (Bedford, OH, USA). Dactinomycin (actinomycin D, MW 1255.43) was purchased from Merck (Whitehouse Station, NJ, USA); its solution was made fresh in dH₂O, and its final concentration was determined by absorbance at 440 nm using an extinction coefficient of 24,450 M^{–1} cm^{–1}. Cisplatin (1 mg/ml, ~3.3 mM in 154 mM NaCl) was purchased from American Pharmaceutical Partners (Schaumburg, IL, USA). Transplatin (yellow powder, MW 300.05) was obtained from Sigma–Aldrich (St. Louis, MO, USA) and dissolved as 1 mg/ml (~3.3 mM) in 0.9% NaCl. Carboplatin (MW 371.25) was purchased as 26.9 mM solution from Mayne Pharma (Paramus, NJ, USA). Oxaliplatin (MW 397.30) was purchased as 12.5 mM solution (50 mg oxaliplatin in 10 ml of dH₂O) from Central Pharmacy. Nedaplatin for injection (MW 303.18) was obtained from Tung Chit Pharmaceutical (Nanjing, China); powder was freshly dissolved in 0.9% NaCl (6.6 mM solution). CsA (MW 1202.64) was purchased from Bedford Laboratories as 41.6 mM solution (250 mg CsA in 5 ml of 33.2% absolute alcohol); a 1:1000 dilution in dH₂O was made before each addition. Tirapazamine (MW 178.15) was obtained from Sanofi–Winthrop (Malvern, PA, USA); its solution was made fresh in dH₂O. NaCN solution (1.0 M) was freshly prepared in dH₂O; the pH was adjusted to approximately 7.0 with 12 N HCl immediately prior to use. RPMI 1640 medium was purchased from Mediatech (Herndon, VA, USA). Caffeine powder (MW 194.19) and remaining reagents were purchased from Sigma–Aldrich.

Cells

Human promyelocytic leukemia (HL-60) and T-cell lymphoma (Jurkat) cells were purchased from American Tissue Culture Collection (Manassas, VA, USA). The cells were cultured in medium plus 10% fetal bovine serum, 1% l-glutamine, and 1% penicillin/streptomycin. Tu183 cells were obtained from Edward J. Shillitoe (State University of New York, Upstate Medical University). They were derived from a squamous cell carcinoma of the tonsil and were highly resistant to therapy. The cells were cultured in Dulbecco's modified Eagle's medium nutrient mixture F-12 (Invitrogen, Carlsbad, CA, USA) plus 10% fetal bovine serum, 1% penicillin/streptomycin, and 0.2% primosin. For harvesting, the cells were incubated at 37 °C in 2.5 ml of 0.05% (w/v) trypsin plus 0.53 mM ethylenediaminetetraacetic acid (EDTA) for 5 min and then collected. Cell counts and viabilities were determined by light microscopy using a hemocytometer under standard trypan blue staining conditions.

Cells were suspended at 0.5 to 1.0 × 10⁶ cells/ml in medium plus 2 μM Pd phosphor and 0.5% fat-free bovine serum albumin. For each condition, 1.0 ml of the cell suspension was placed in a 1-ml glass vial (8-mm clear vials, Krackler Scientific, Albany, NY, USA). The vial was sealed with a crimp top aluminum seal (using a Wheaton hand crimper, Fisher Scientific) and placed in the instrument for O₂ measurement at 37 °C. Mixing was accomplished with the aid of parylene-coated stirring bars (1.67 × 2.01 × 4.8 mm, V&P Scientific, San Diego, CA, USA).

O₂ measurement

The O₂ detection system was built to measure the phosphorescence of Pd phosphor as described previously [21,22]. DASYlab (Measurement Computing, Norton, MA, USA) was used for data acquisition. The data were analyzed by a C++ language computing program [25] that calculated phosphorescence lifetime (τ) and decay constant (1/τ). Because oxygen quenches the phosphorescence, the decay rate 1/τ is a linear function of [O₂] as

$$1/\tau = 1/\tau_0 + k_q[\text{O}_2],$$

where 1/τ₀, the decay rate in the absence of oxygen, was 10,087 ± 156 s^{–1} and the value of the quenching rate constant, k_q, was 96.1 ± 1.2 μM^{–1} s^{–1} [21].

Index of respiration inhibition

Here we propose an index for the efficiency with which a chemical agent inhibits cellular respiration. The index can be calculated from a graph of [O₂] versus *t* when [O₂] is measured in a closed container because the negative of the slope, –d[O₂]/dt, is the respiration rate *k* (considered as a zero-order rate constant). For cells not treated by cytotoxic agents, *k* is a constant, so that [O₂] is a linear function of time,

$$[\text{O}_2] = [\text{O}_2]_0 - kt. \quad (1)$$

The initial concentration of oxygen, [O₂]₀, can be calculated from the Henry's law constant for O₂, assuming that the solution is saturated with air ([O₂]₀ is 225 μM for 37 °C). For cells treated with most drugs, the value of *k* is time dependent; that is, [O₂] does not decrease linearly with time. Therefore, we propose to calculate the average value of *k* over a fixed time interval from experimental measurements of [O₂] versus *t*,

$$\langle k \rangle \equiv \frac{1}{t_f - t_i} \int_{t_i}^{t_f} k dt,$$

and use $\langle k \rangle$ as a measure of cytotoxicity. Because $k = -d[O_2]/dt$,

$$\langle k \rangle = \frac{[O_2]_i - [O_2]_f}{t_f - t_i} \quad (2)$$

Because of the fluctuations in measured $[O_2]$, one cannot simply use the measured $[O_2]$ values at the end points of the interval to calculate $\langle k \rangle$. Rather, one should use all of the measured values in the calculation of $\langle k \rangle$.

To do this, we fit all of the measurements to a suitable analytic function and calculate $[O_2]$ at the end points from the parameterized function. A simple and convenient fitting function is a second-order polynomial, $[O_2] = \alpha + \beta t + \gamma t^2$. This is appropriate because it includes the linear function as a special case, $\gamma = 0$. With this function, $k = -(\beta + 2\gamma t)$ and $\langle k \rangle = -\beta - \gamma(t_i + t_f)$. It is expected that the quadratic will be concave upward, corresponding to a gradual decrease in respiration rate, so that β will be negative and γ will be positive. More generally, a power series, $[O_2] = a + bt + ct^2 + dt^3 \dots$, can be adopted. If the parameters c and d are small, $[O_2]$ versus t will be a line; if not, it will be curved. The cubic term makes it possible to represent a k that is nonmonotonic in time. Although we have not found any cases where the fit is improved significantly by going past the t^2 term, this must be checked under specific circumstances. The average value of k for the cubic is

$$\langle k \rangle = \frac{\int_{t_i}^{t_f} k dt}{\int_{t_i}^{t_f} dt} = \frac{-1}{t_f - t_i} \int_{t_i}^{t_f} (b + 2ct + 3dt^2) dt$$

$$= -b - c(t_f + t_i) - d(t_f^2 + t_f t_i + t_i^2). \quad (3)$$

For all toxin-treated conditions, we choose $t_f - t_i$ as a fixed time interval. Invariably, t_i is longer than the preceding incubation time by the time required for the sample preparation. In our experiments, this time can vary from a few minutes to a half-hour, depending on the number of sampling conditions, and is different for different samples. However, this does not affect the calculation of $\langle k \rangle$ given that $\langle k \rangle$ is an average over the same time period for all samples.

After the calculation of $\langle k \rangle$ from fitting of the experimental data to a polynomial, we propose to calculate an index, I , defined as

$$I = 1 - \frac{\langle k \rangle}{\langle k \rangle_0}, \quad (4)$$

where $\langle k \rangle$ is the average value of negative slope in the toxin-treated condition and $\langle k \rangle_0$ is the average value of negative slope in the untreated condition. The meaning of I is the average inhibition of cellular respiration due to the toxin treatment during the period when measurements are made. If I depends on dosage D , experimentally determined I values can be fitted to the function

$$I = \left[\frac{D}{A + D} \right] \cdot I_{\max}, \quad (5)$$

where I_{\max} and A are constants for a particular drug and cell line. When drug dosage reaches the concentration A , I equals half-maximal inhibition (I_{\max}) of cellular respiration.

When a polynomial is used to fit experimental $[O_2]$ for $t_i < t < t_f$, it must be remembered that the polynomial has no validity outside this region (e.g., $[O_2]$ certainly does not increase rapidly for later t as a quadratic does). Because the polynomial cannot be used to extrapolate to $t = 0$, it may be necessary to use the initial $[O_2]$ (e.g., 225 μM at 37 °C). This information is added to the experimental points before fitting.

Results

Dactinomycin and doxorubicin

We first evaluated the impact of a prolonged exposure to dactinomycin or doxorubicin on cellular respiration. HL-60 cells

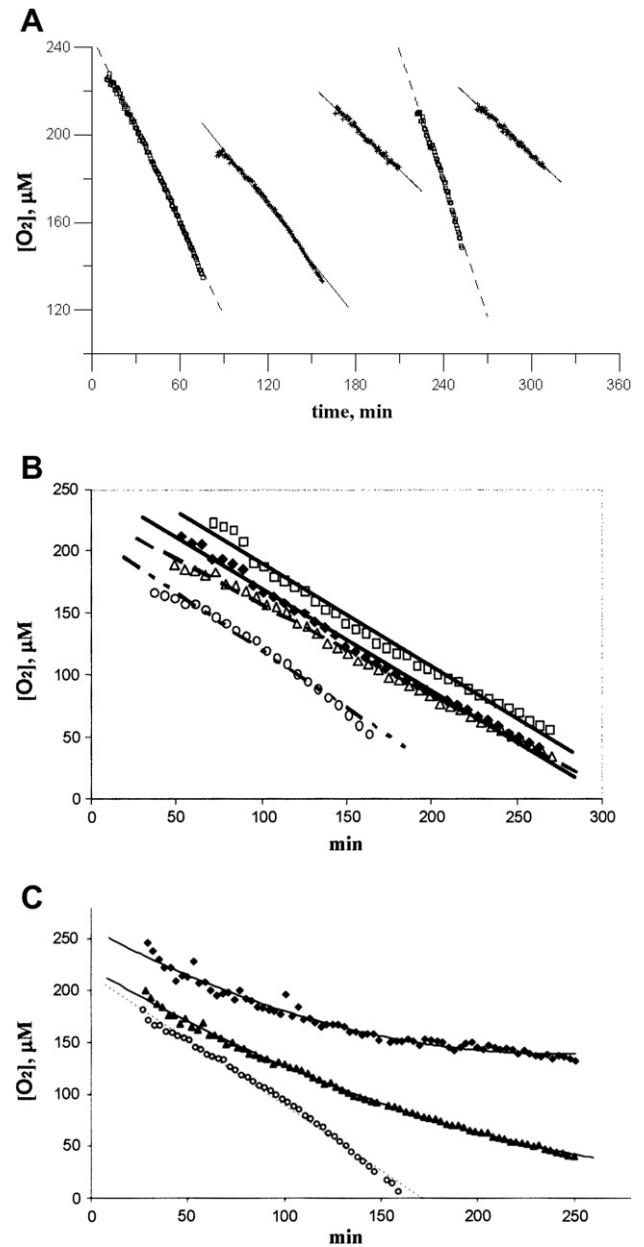


Fig. 1. (A) Effects of dactinomycin on cellular respiration. HL-60 cells (10^6 cells/ml) were suspended in medium, 2 μM Pd phosphor, and 0.5% bovine serum albumin with 10 μM dactinomycin (plus signs) or without drug (open circles). Time zero corresponds to the addition of dactinomycin. The cells were then placed in the 37 °C incubator. Aliquots (1.0 ml each) of untreated and treated cells were taken periodically for $[O_2]$ measurement, performed every 30 s. Linear fits were made to the data for each condition (dashed lines for untreated cells, solid lines for treated cells). (B) Effect of combined dactinomycin plus doxorubicin on cellular respiration. Jurkat cells (0.5×10^6 cells/ml) were suspended in medium, 2 μM Pd phosphor, and 0.5% albumin without drug addition (open circles) or with the addition of 20 μM dactinomycin (open triangles), 20 μM doxorubicin (open squares), or 10 μM dactinomycin + 10 μM doxorubicin (filled diamonds). Time zero corresponds to the addition of drugs. Each vial was taken sequentially (every 60 s) for respiration measurement. Linear fits were made to the data for each condition (dashed lines for cells untreated or treated with dactinomycin only, solid lines for cells treated with doxorubicin or both drugs). (C) Effect of dactinomycin on cellular respiration. Jurkat cells (0.5×10^6 cells/ml) were suspended in medium, 2 μM Pd phosphor, and 0.5% albumin without drug addition (open circles) or with the addition of 10 μM dactinomycin (filled triangles) or 20 μM dactinomycin (filled diamonds). $[O_2]$ was measured alternately every minute on the three conditions. Linear fits to the data set for untreated cells are dashed lines, and quadratic fits to dactinomycin data sets are solid lines.

(10^6 cells/ml) were suspended in medium, 2 μ M Pd phosphor, and 0.5% bovine serum albumin without or with 10 μ M dactinomycin. The suspensions were then placed in the 37 °C incubator. Aliquots (1.0 ml each) of untreated and treated cells were taken periodically for $[O_2]$ measurement, with $[O_2]$ being determined every 30 s. Measured $[O_2]$ is shown as a function of time in Fig. 1A (open circles for untreated cells, plus signs for treated cells). Time zero corresponds to the addition of dactinomycin or the beginning of incubation. First, a sample of untreated cells was run for approximately 75 min, and then it was replaced by a sample of drug-treated cells that was run for approximately 50 min. Thereafter, samples of untreated and treated cells were run. For each run, it was found that $[O_2]$ decreased linearly with t , so $[O_2]$ versus t was fit to a line (dotted for untreated cells, solid for treated cells) in each case.

The values of k for the two measurements on untreated cells, at 0 and 210 min, were 1.42 and 1.99 μ M O_2 /min, respectively ($r^2 = 0.998$ and 0.991, respectively). The increase in respiration rate with time for untreated cells was attributed to cell growth. We assume that, in the absence of drug, k for untreated cells increases linearly (i.e., $k = 1.42 + (1.99 - 1.42)t/210$), so that at 90, 150, and 270 min, $k = 1.66, 1.83,$ and 2.15μ M O_2 /min, respectively. The values of k for the three measurements on treated cells (Fig. 1A) were 0.846, 0.642, and 0.639 μ M O_2 /min ($r^2 = 0.993, 0.986,$ and 0.986), respectively. Thus, respiration was inhibited by 49% at 90 min, by 65% at 150 min, and by 70% at 270 min, showing that dactinomycin treatment caused progressive inhibition of respiration (see Table 1).

In another protocol, measurements of $[O_2]$ were made alternatively every 60 s on all of the samples (i.e., going to a different sample every 60 s) using the therapeutic drug doxorubicin as well as dactinomycin. Jurkat cells (0.5×10^6 cells/ml) were suspended in medium, 2 μ M Pd phosphor, and 0.5% albumin without drug addition (open circles) or with the addition of 20 μ M dactinomycin (open triangles), 20 μ M doxorubicin (open squares), or 10 μ M dactinomycin plus 10 μ M doxorubicin (filled diamonds) (Fig. 1B). Time zero corresponds to the drug addition (beginning of incubation),

and measurements began at 50 min, so that incubation time was 50 min.

Linear fits were made to the data for each condition (dashed lines for untreated and dactinomycin-treated cells, solid lines for doxorubicin-treated cells and cells treated with both drugs). The slopes were -0.929μ M O_2 /min for untreated cells ($r^2 = 0.984$), -0.732μ M O_2 /min for dactinomycin-treated cells ($r^2 = 0.996$), -0.833μ M O_2 /min for doxorubicin-treated cells ($r^2 = 0.987$), and -0.826μ M O_2 /min for the mixture ($r^2 = 0.995$). Because deviations from linearity were not evident, calculation of average k was unnecessary. For the three conditions, respiration decreased by 21, 10, and 11%, respectively. The results show that for Jurkat cells, dactinomycin is more potent than doxorubicin and the effect of combining the two drugs is less than additive.

The advantages of this protocol include the ability to compare multiple conditions (the same drug at different dosages or the same dosage for various drugs) synchronously. Also, this protocol requires fewer cells per condition, allowing lower rates of O_2 consumption and, thus, longer measurement times that may permit detection of deviations from linearity in $[O_2]$ versus t . Based on the above experience, we adopted the latter protocol in most of our experiments.

We previously reported [21] that $[O_2]$ versus t plots for cells treated with doxorubicin were actually well fit by two lines; that is, k was constant and equal to the value for untreated cells for approximately 150 min and then decreased to a lower value. The results of Fig. 1B may show this discontinuity in slope. However, this does not have a major effect on our conclusions given that the k values from linear fits, reported above, are average values for the full time of measurement. In contrast to doxorubicin, dactinomycin produced nonlinear $[O_2]$ versus t plots that were concave upward; that is, k decreased gradually with time [22]. Therefore, dactinomycin data for long periods of time should be analyzed using a polynomial model.

Fig. 1C shows $[O_2]$ versus t for 0.5×10^6 Jurkat cells/ml under the same conditions as for Figs. 1A and 1B. Open circles represent

Table 1
Values of k for cisplatin-treated and untreated cells and r^2 values

Condition	Cell type and concentration	Drug	Concentration (μ M)	Incubation time (min)	k (μ M O_2 /min), untreated	k (μ M O_2 /min), treated	Ratio of k values
1	HL-60, 10^6 /ml	Dactinomycin	10	90	1.660	0.846	0.510
2	HL-60, 10^6 /ml	Dactinomycin	10	150	1.830	0.642	0.350
3	HL-60, 10^6 /ml	Dactinomycin	10	270	2.150	0.639	0.300
4	Jurkat, 0.5×10^6 /ml	Dactinomycin	20	50	0.929	0.732	0.790
5	Jurkat, 0.5×10^6 /ml	Doxorubicin	20	50	0.929	0.833	0.900
6	Jurkat, 0.5×10^6 /ml	Dactinomycin + doxorubicin	10 + 10	50	0.929	0.826	0.890
7	Jurkat, 0.5×10^6 /ml	Dactinomycin	10	30	1.252	0.898	0.717
8	Jurkat, 0.5×10^6 /ml	Dactinomycin	10	90	1.252	0.608	0.486
9	Jurkat, 0.5×10^6 /ml	Dactinomycin	10	150	1.252	0.368	0.294
10	Jurkat, 0.5×10^6 /ml	Dactinomycin	10	210	1.252	0.128	0.102
11	Jurkat, 0.5×10^6 /ml	Dactinomycin	20	30	1.252	0.793	0.633
12	Jurkat, 0.5×10^6 /ml	Dactinomycin	20	90	1.252	0.553	0.442
13	Jurkat, 0.5×10^6 /ml	Dactinomycin	20	150	1.252	0.313	0.250
14	Jurkat, 0.5×10^6 /ml	Dactinomycin	20	210	1.252	0.073	0.058
15	Jurkat, 0.5×10^6 /ml	Doxorubicin	3	90	1.144	1.002	0.876
16	Jurkat, 0.5×10^6 /ml	Doxorubicin	3	150	1.144	0.692	0.604
17	Jurkat, 0.5×10^6 /ml	Doxorubicin	5	90	1.144	0.947	0.828
18	Jurkat, 0.5×10^6 /ml	Doxorubicin	5	150	1.144	0.650	0.656
19	Jurkat, 0.5×10^6 /ml	Doxorubicin	10	90	1.144	0.886	0.774
20	Jurkat, 0.5×10^6 /ml	Doxorubicin	10	150	1.144	0.619	0.541
21	Jurkat, 0.5×10^6 /ml	Doxorubicin	20	90	1.144	0.795	0.696
22	Jurkat, 0.5×10^6 /ml	Doxorubicin	20	150	1.144	0.354	0.309
23	Jurkat, 0.5×10^6 /ml	Doxorubicin	40	90	1.144	0.773	0.676
24	Jurkat, 0.5×10^6 /ml	Doxorubicin	40	150	1.144	0.457	0.399
25	HL-60, 0.5×10^6 /ml	Dactinomycin	10	30	0.645	0.559	0.867
26	HL-60, 0.5×10^6 /ml	Dactinomycin	10	180	0.435	0.228	0.524
27	HL-60, 0.5×10^6 /ml	Doxorubicin	20	30	0.645	0.503	0.780
28	HL-60, 0.5×10^6 /ml	Doxorubicin	20	180	0.435	0.223	0.513

untreated cells, filled triangles represent cells treated with 10 μM dactinomycin, and filled diamonds represent cells treated with 20 μM dactinomycin. All of the data for untreated cells were well fit to a line ($r^2 = 0.994$) as expected. The slope was $-1.252 \mu\text{M}/\text{min}$, and the y intercept was $214.7 \mu\text{M}$. The linear fit for 10 μM drug-treated cells is $[\text{O}_2] = 227.7 \mu\text{M} - (0.420 \mu\text{M}/\text{min})t$ ($r^2 = 0.982$); for 20 μM drug-treated cells, $[\text{O}_2] = 198.6 \mu\text{M} - (0.674 \mu\text{M}/\text{min})t$ ($r^2 = 0.899$). Obviously, both poor linear fits show that curvature is important, so that quadratic fits (shown as solid lines) are a big improvement. For 10 μM drug-treated cells, the quadratic is $[\text{O}_2] = 221.0 \mu\text{M} - (1.088 \mu\text{M}/\text{min})t + (0.002 \mu\text{M}/\text{min}^2)t^2$ ($r^2 = 0.998$), so that $\beta = -1.088 \mu\text{M}/\text{min}$ and $\gamma = 0.002 \mu\text{M}/\text{min}^2$. For 20 μM drug-treated cells, $[\text{O}_2] = 259.6 \mu\text{M} - (1.003 \mu\text{M}/\text{min})t + (0.002 \mu\text{M}/\text{min}^2)t^2$ ($r^2 = 0.972$). We take $t_i = 30, 90, 150,$ and 210 min and $t_f - t_i = 60$ min for all four cases. Then $\langle k \rangle$ is calculated as $-\beta - \gamma(t_i + t_f)$ for all eight cases, giving the results in Table 1 (lines 7–14). For each t_i , the inhibition is greater for the higher drug concentration; for each drug concentration, the inhibition increases with time.

The same method was employed to analyze the next experiments on doxorubicin-treated cells. Altered O_2 consumption profiles due to treatment with doxorubicin at various doses are shown in Fig. 2A. Here 0.5×10^6 Jurkat cells/ml were treated with 0 μM doxorubicin (open circles), 3 μM doxorubicin (open triangles), 5 μM doxorubicin (open squares), 10 μM doxorubicin (filled triangles), 20 μM doxorubicin (filled diamonds), and 40 μM doxorubicin (filled squares). For all drug-treated conditions, $[\text{O}_2]$ was measured out to 200 min. The point at $t = 0, [\text{O}_2] = 225 \mu\text{M}$, calculated for air-saturated dH_2O , was added to the measured points. As shown in Fig. 2A, the O_2 consumption profiles for doxorubicin-treated conditions were fitted to quadratic forms, and the profile for untreated cells was fitted to a line (constant k value). The value of k for untreated cells, the negative of the slope of the best-fit line, was $1.144 \mu\text{M}/\text{min}$ ($r^2 = 0.988$).

For cells treated with 3, 5, 10, 20, or 40 μM doxorubicin, least-squares fitted to quadratics, the values of the linear and quadratic coefficients β and γ were as follows: for 3 μM drug, $\beta = -1.504$ and $\gamma = 0.0022$ ($r^2 = 0.996$); for 5 μM drug, $\beta = -1.341$ and $\gamma = 0.0016$ ($r^2 = 0.998$); for 10 μM drug, $\beta = -1.420$ and $\gamma = 0.0022$ ($r^2 = 0.988$); for 20 μM drug, $\beta = -1.681$ and $\gamma = 0.0037$ ($r^2 = 0.988$); for 40 μM drug, $\beta = -1.406$ and $\gamma = 0.0026$ ($r^2 = 0.979$). Values of $\langle k \rangle$ were then calculated from the quadratic forms, with $t_i = 30, 90, 150,$ and 210 min and $t_f - t_i = 60$ min, as for dactinomycin. The values are given in Table 1 for $t_i = 90$ and 150 min only. This is sufficient because if a single quadratic is used to fit all of the data for $[\text{O}_2]$ versus t , $\langle k \rangle$ will be a linear function of t_i so long as $t_f - t_i$ is kept constant.

Calculated inhibitions (values of I) are plotted in Fig. 2B. It should be noted that results for 40 μM doxorubicin are less reliable than results for other concentrations because $d[\text{O}_2]/dt$ becomes zero (100% inhibition) before the time of measurement, which is 200 min. Also shown in Fig. 2B is the best fit ($r^2 = 0.933$) of I to Eq. (5). The best values for I_{max} and A are 0.735 and $3.27 \mu\text{M}$, respectively. We also fitted to Eq. (5) with $I_{\text{max}} = 1$ (i.e., 100% inhibition) and found the best value of A (8.45 M). However, the low value of r^2 (0.817) indicated that the latter fitting was not suitable.

The results presented so far indicate that dactinomycin is approximately twice as potent as doxorubicin for Jurkat cells; that is, to get comparable inhibition of respiration, doxorubicin must be used at twice the concentration of dactinomycin. We next investigated the effect of these two drugs on HL-60 cell respiration. We incubated 0.5×10^6 HL-60 cells/ml in open containers without or with 10 μM dactinomycin or 20 μM doxorubicin. A 1.0-ml aliquot for untreated and treated cells was taken every 150 min for O_2 measurement. Fig. 2C shows the results for untreated cells (open circles), 10 μM dactinomycin-treated cells (filled triangles), and

20 μM doxorubicin-treated cells (filled squares). The incubation time for each set of measurements is the time of the first measurement (i.e., 30 min for the first three runs and 180 min for the second three runs). Because each set of measurements was over a limited time, the k values were obtained from the best linear fits. At $t = 30$ min, $k = 0.645 \mu\text{M O}_2/\text{min}$ for untreated cells ($r^2 = 0.993$), $0.559 \mu\text{M O}_2/\text{min}$ for dactinomycin-treated cells ($r^2 = 0.989$), and $0.503 \mu\text{M O}_2/\text{min}$ for doxorubicin-treated cells ($r^2 = 0.989$); at $t = 180$ min, $k = 0.435 \mu\text{M O}_2/\text{min}$ for untreated cells ($r^2 = 0.996$), $0.228 \mu\text{M O}_2/\text{min}$ for dactinomycin-treated cells ($r^2 = 0.967$), and $0.223 \mu\text{M O}_2/\text{min}$ for doxorubicin-treated cells ($r^2 = 0.903$). Thus, after 30 min incubation, dactinomycin inhibited HL-60 cell respira-

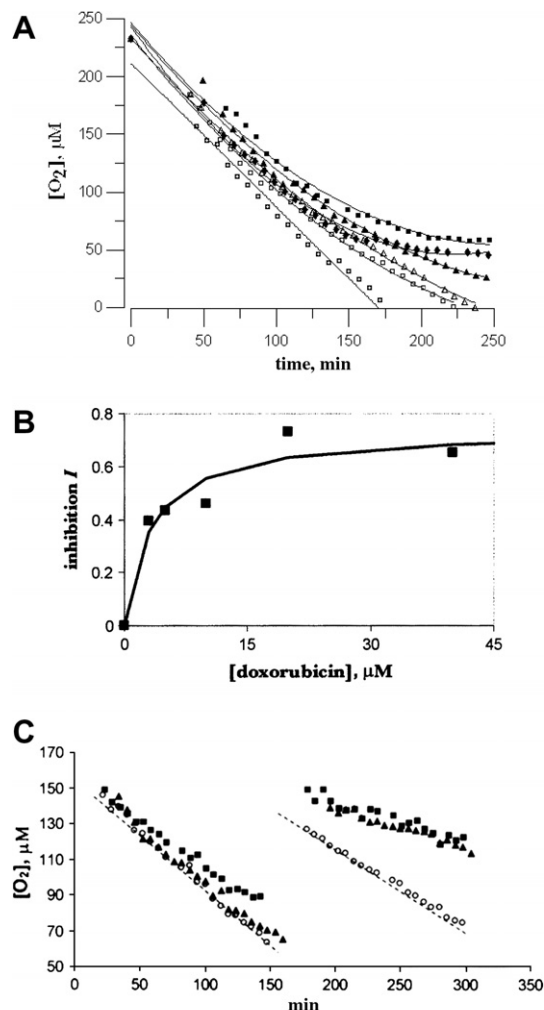


Fig. 2. (A) Measurement of respiration rate. Jurkat cells (0.5×10^6 cells/ml) were suspended in medium, 2 μM Pd phosphor, and 0.5% bovine serum albumin without drug treatment (open circles) or with treatment with 3 μM doxorubicin (open squares), 5 μM doxorubicin (open triangles), 10 μM doxorubicin (filled triangles), 20 μM doxorubicin (filled diamonds), or 40 μM doxorubicin (filled squares). Quadratic fits for all doxorubicin-treated conditions are shown as indicated; the data for untreated cells were fit to a line. The respiration rates are obtained as the negative derivatives, $k = -d[\text{O}_2]/dt$. (B) Values of average k at 150 min incubation were calculated from the quadratic fits (linear fit for untreated cells), and inhibition I was calculated for each concentration. Values of I are plotted versus $[\text{doxorubicin}]$ (filled squares) and compared with best-fit function (line). The function is $I = I_{\text{max}}D / (A + D)$, where D is drug concentration, $I_{\text{max}} = 0.735$, and $A = 3.27 \mu\text{M}$ ($r^2 = 0.933$). (C) HL-60 cells (0.5×10^6 cells/ml) were suspended in medium, 2 μM Pd phosphor, and 0.5% albumin without drug treatment (open circles) or with treatment with 10 μM dactinomycin (filled triangles) or 20 μM doxorubicin (filled squares). Time zero corresponds to the addition of drugs. Aliquots (1.0 ml each) of untreated and treated samples were taken every 150 min for O_2 measurement. Dashed lines show the best linear fits for untreated cell respiration.

tion by 13.3%, whereas doxorubicin inhibited respiration by 22.0%; after 180 min incubation, dactinomycin inhibited cell respiration by 47.6%, whereas doxorubicin inhibited respiration by 48.8%. Thus, dactinomycin is twice as potent as doxorubicin for HL-60 cells as well as for Jurkat cells.

There is an apparent decrease in the respiration rate for untreated cells with time ($k = 0.645$ at 30 min and 0.435 at 180 min), possibly due to problems with maintenance of the cell culture. Day-to-day variations are likely even more important than intraday variations. This underlines the importance of always comparing measured k for treated cells with k for untreated cells from the same batch measured over the same time period, as we did here.

Pt compounds

We next investigated the effects of Pt compounds on the respiration of Jurkat cells. Fig. 3A shows results of one experiment in which 10^6 cells/ml were untreated (open circles) or were treated with $20 \mu\text{M}$ cisplatin (filled squares), carboplatin (filled triangles), oxaliplatin (filled diamonds), or nedaplatin (filled circles) or with 10 mM NaCN (crosses). The values of k were obtained from the best linear fits and were as follows (means \pm standard deviations from the best linear fits): $1.54 \pm 0.05 \mu\text{M O}_2/\text{min}$ for untreated cells ($r^2 > 0.984$), $1.66 \pm 0.05 \mu\text{M O}_2/\text{min}$ for cisplatin-treated cells

($r^2 > 0.987$), $1.50 \pm 0.06 \mu\text{M O}_2/\text{min}$ for carboplatin-treated cells ($r^2 > 0.977$), $1.53 \pm 0.06 \mu\text{M O}_2/\text{min}$ for oxaliplatin-treated cells ($r^2 > 0.980$), $1.61 \pm 0.07 \mu\text{M O}_2/\text{min}$ for nedaplatin-treated cells ($r^2 > 0.976$), and $0.27 \pm 0.05 \mu\text{M O}_2/\text{min}$ for the cyanide-treated condition ($r^2 > 0.660$). Thus, the average rate of cellular respiration under treatment of different Pt drugs was $1.58 \pm 0.07 \mu\text{M O}_2/\text{min}$, which was the same as that for individual drugs within statistical error. Furthermore, the rate of respiration for drug-treated cells was not statistically different from the rate for untreated cells within statistical error. The plots for the drug-treated cells showed no systematic deviation from linearity, confirming that none of the drugs inhibited respiration during the 100 min when $[\text{O}_2]$ was measured. In contrast, the addition of NaCN inhibited cellular respiration 82.5% during the 100 min incubation. On performing the same experiments with all of the Pt compounds but changing the cell line to Tu183 and HL-60 cells, similar results were observed; that is, there was no inhibition occurring in Pt drug-treated cell respiration after approximately 2 h exposure.

The next experiment was performed to confirm and extend the above observations. Jurkat cells (0.5×10^6 cells/ml) were incubated without or with $40 \mu\text{M}$ cisplatin. Aliquots (1.0 ml each) from untreated and treated samples were taken every 180 min for O_2 measurement. Fig. 3B shows the results for untreated cells (open circles) and $40 \mu\text{M}$ cisplatin-treated cells (filled squares), with the dashed lines being the best linear fits for untreated cells. The

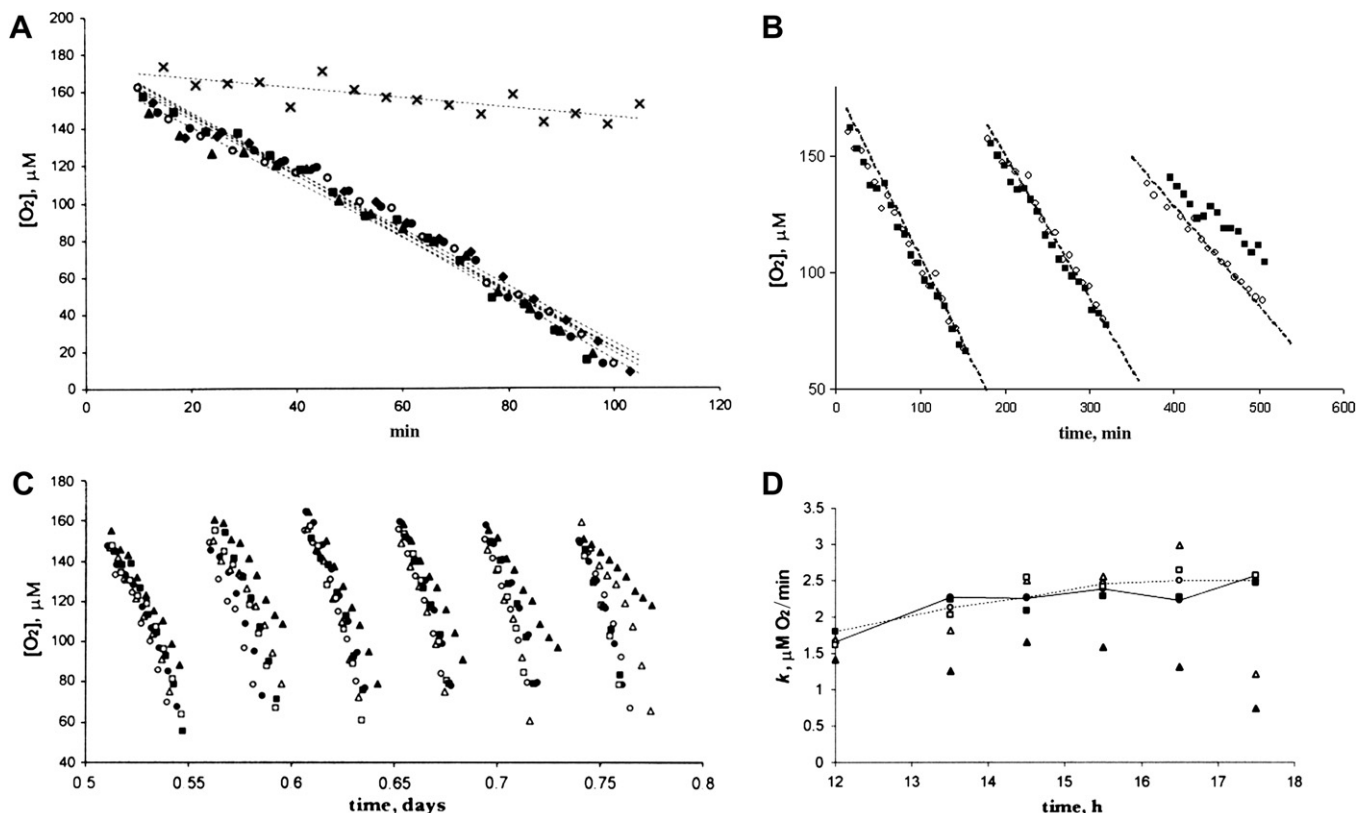


Fig. 3. Effects of Pt compounds on Jurkat cells. Jurkat cells ($0.5\text{--}1.0 \times 10^6$ cells/ml) were suspended in medium containing $2 \mu\text{M}$ Pd phosphor and 0.5% bovine serum albumin. (A) Here 1.0×10^6 Jurkat cells/ml were untreated (open circles) or were treated with $20 \mu\text{M}$ cisplatin (filled squares), $20 \mu\text{M}$ carboplatin (filled triangles), $20 \mu\text{M}$ oxaliplatin (filled diamonds), or $20 \mu\text{M}$ nedaplatin (filled circles) or with 10 mM NaCN (crosses). Linear fits for all conditions are shown as dashed lines. (B) Here 0.5×10^6 Jurkat cells/ml were untreated (open circles) or were treated with $40 \mu\text{M}$ cisplatin (filled squares). Time zero corresponds to the addition of drugs. Aliquots (1.0 ml) of untreated and treated samples were taken every 3 h for O_2 measurement. Dashed lines indicate the best linear fits for untreated cell respiration. (C) Here 0.5×10^6 Jurkat cells/ml were untreated (duplicates, open or filled circles) or were treated with 20 or $40 \mu\text{M}$ cisplatin (open or filled triangles) or 20 or $40 \mu\text{M}$ transplatin (open or filled squares). Time zero corresponds to the addition of drugs. After 12 h incubation, 1.0-ml aliquots of untreated and treated samples were taken every 60 or 90 min for O_2 measurement. All of the k values, obtained from the best linear fits, are given in Table 2. (D) All of the k values (in $\mu\text{M O}_2/\text{min}$) in Table 1 are plotted versus incubation time before sampling. Duplicate results for untreated cells are open or filled circles connected by lines, results for cells treated with 20 or $40 \mu\text{M}$ cisplatin are open or filled triangles, and results for cells treated with transplatin are open or filled squares. Time zero corresponds to the addition of drugs; cells were continuously exposed up to the time of sampling for O_2 measurements.

Table 2Values of k for cisplatin-treated and untreated cells and r^2 values

Condition	k ($\mu\text{M O}_2/\text{min}$)					
	12.0 h exposure	13.5 h exposure	14.5 h exposure	15.5 h exposure	16.5 h exposure	17.5 h exposure
Untreated 1	1.80 (0.962)	2.19 (0.972)	2.05 (0.963)	2.33 (0.985)	2.32 (0.983)	2.26 (0.958)
Untreated 2	1.59 (0.974)	2.00 (0.951)	2.11 (0.985)	2.22 (0.975)	2.08 (0.968)	2.34 (0.974)
20 μM cisplatin	1.68 (0.987)	1.81 (0.979)	2.32 (0.977)	2.37 (0.975)	2.70 (0.950)	1.49 (0.960)
40 μM cisplatin	1.36 (0.992)	1.07 (0.947)	1.54 (0.966)	1.45 (0.992)	1.31 (0.989)	0.71 (0.988)
20 μM transplatin	1.61 (0.960)	1.81 (0.969)	2.54 (0.972)	2.41 (0.987)	2.64 (0.990)	2.57 (0.975)
40 μM transplatin	1.80 (0.951)	2.06 (0.989)	2.08 (0.961)	2.29 (0.973)	2.27 (0.966)	2.47 (0.986)

Note: r^2 values are in parentheses.

k values were as follows: at $t = 0$ min, $0.666 \mu\text{M O}_2/\text{min}$ for untreated cells ($r^2 = 0.987$) and $0.690 \mu\text{M O}_2/\text{min}$ for cisplatin-treated cells ($r^2 = 0.992$); at $t = 180$ min, $0.572 \mu\text{M O}_2/\text{min}$ for untreated cells ($r^2 = 0.983$) and $0.580 \mu\text{M O}_2/\text{min}$ for cisplatin-treated cells ($r^2 = 0.991$); at $t = 440$ min, $0.354 \mu\text{M O}_2/\text{min}$ for untreated cells ($r^2 = 0.990$) and 0.343 for cisplatin-treated cells ($r^2 = 0.936$). Here again, the respiration rates in untreated cells decline as time elapses. However, there is no statistically significant difference in cellular O_2 consumption rates between treated and untreated cells for up to 6 h continuous exposure to $40 \mu\text{M}$ cisplatin.

In the next series of experiments, we incubated Jurkat cells (0.5×10^6 cells/ml) suspended in medium (containing $2 \mu\text{M}$ Pd phosphor and 0.5% bovine serum albumin) with 20 or $40 \mu\text{M}$ cisplatin for 12 h. At the same time, a culture of the same cells was maintained with no cisplatin added and, as a further control, a culture of the same cells was incubated with 20 - or 40 - μM concentrations of transplatin. After 12 h, aliquots (1.0 ml each) of untreated and treated samples were taken periodically for O_2 measurement. To check reproducibility, duplicate samples were taken of the untreated cells. Oxygen measurements were stopped and a new set of aliquots was taken when $[\text{O}_2]$ in a sample of untreated cells reached $50 \mu\text{M}$. This almost always meant a new set every hour. Results are shown in Fig. 3C.

The k values obtained from the best linear fits are shown in Table 2 and plotted versus sampling start time (which is equal to incubation time) in Fig. 3D. It is clear that k values in duplicate untreated cell samples (open or filled circles, connected by lines) stay close to each other, confirming that the measurements are consistent and repeatable. Overall, k values for untreated cells increase with time. The increase in k with time is ascribed to cell growth. Cells treated with $20 \mu\text{M}$ transplatin (open squares) or $40 \mu\text{M}$ transplatin (filled squares) show no difference from the untreated cells, suggesting that 18 h continuous exposure to transplatin has no inhibitory effect on cellular respiration.

For $20 \mu\text{M}$ cisplatin-treated cells, respiration rate remained similar to that for untreated cells up to 17 h and then decreased. This result agrees with a previous study on cisplatin-induced caspase activation in Jurkat cells, where caspase activity started at 14 h incubation with $20 \mu\text{M}$ cisplatin [23]. For $40 \mu\text{M}$ cisplatin-treated Jurkat cells, respiration rates appear to be significantly lower than those for untreated cells after 12 h, implying that the inhibition of mitochondrial O_2 consumption occurred earlier for the higher concentration. The decrease in respiration is more marked after 15 h. The inhibition I may be calculated as 1 minus the ratio of k for treated cells to k for untreated cells (with the average of two values being used for untreated cells). Then, for the incubation times in Table 3, the values of I with $20 \mu\text{M}$ cisplatin are 0.01 , 0.14 , -0.12 , -0.04 , -0.23 , and 0.35 . For $40 \mu\text{M}$ cisplatin, $I = 0.20$, 0.48 ,

0.26 , 0.36 , 0.40 , and 0.69 . These results reflect a dose-dependent and time-dependent inhibition of cellular respiration by cisplatin, whereas there is no observable impairment by the trans-isomer.

Tirapazamine

We first studied the effect of tirapazamine in low concentrations (0 – $15 \mu\text{M}$) on HL-60 cell respiration, with 0.5×10^6 cells/ml being incubated with 0 , 1 , 3 , 5 , 10 , and $15 \mu\text{M}$ drug. Fig. 4A shows the respiratory profiles for untreated cells (open circles) and for cells treated with $1 \mu\text{M}$ tirapazamine (filled squares), $3 \mu\text{M}$ tirapazamine (filled triangles), $5 \mu\text{M}$ tirapazamine (filled diamonds), $10 \mu\text{M}$ tirapazamine (filled circles), or $15 \mu\text{M}$ tirapazamine (open squares) in 3 h exposure. Results for untreated cells were fitted to a line with a slope of $-0.487 \mu\text{M}/\text{min}$ (best linear fitting, dashed line). Results for treated cells, which did not suggest curvature, were also fitted to lines. Quadratic fitting improves r^2 only in the fourth decimal place. The k values obtained from the best linear fits for 0 , 1 , 3 , 5 , 10 , and $15 \mu\text{M}$ tirapazamine ($r^2 = 0.995$, 0.935 , 0.986 , 0.966 , 0.974 , and 0.991 , respectively) are given in the first six lines of Table 3. There is no statistically significant trend in the values of $\langle k \rangle / \langle k_0 \rangle$, although they are all significantly lower than unity. Thus, the effect of tirapazamine at these concentrations is too small to be accurately measured.

To study the effect of higher concentrations of tirapazamine on HL-60 cell respiration, 10^6 cells/ml were incubated with various concentrations of the drug for 3 h. Fig. 4B shows O_2 consumption

Table 3

Average respiration rates for tirapazamine-treated HL-60 cells

[Drug] (μM)	Incubation time (min)	$\langle k \rangle$ ($\mu\text{M}/\text{min}$)	$\langle k \rangle / \langle k_0 \rangle$
0	90	0.4870	—
1	90	0.3750	0.770
3	90	0.3820	0.784
5	90	0.3960	0.811
10	90	0.3740	0.768
15	90	0.4300	0.883
0	90	0.6444	—
0	150	0.3745	—
50	90	0.5770	0.895
50	150	0.2454	0.655
100	90	0.5356	0.831
100	150	0.2937	0.784
200	90	0.5967	0.926
200	150	0.3419	0.913
500	90	0.5180	0.804
500	150	0.2084	0.749
1000	90	0.4106	0.637
1000	150	0.2223	0.594

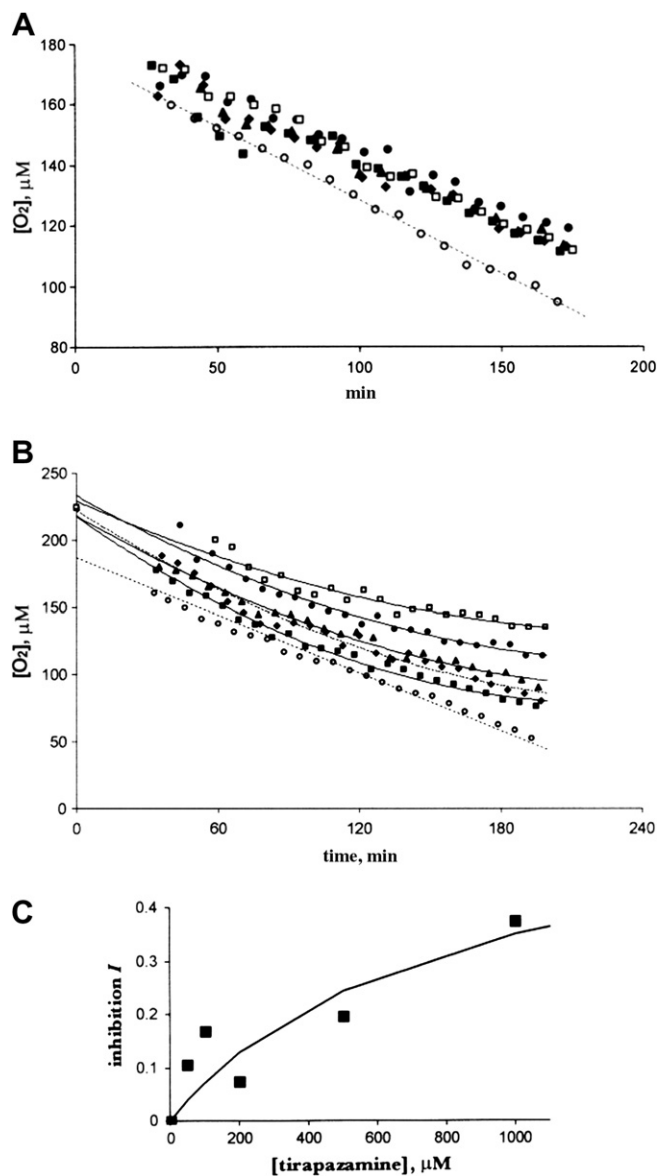


Fig. 4. Effects of tirapazamine on cellular respiration of HL-60 cells suspended in medium containing 2 μM Pd phosphor and 0.5% bovine serum albumin. (A) HL-60 cells (0.5×10^6 cells/ml) were incubated without drug (open circles) or with 1 μM tirapazamine (filled squares), 3 μM tirapazamine (filled triangles), 5 μM tirapazamine (filled diamonds), 10 μM tirapazamine (filled circles), or 15 μM tirapazamine (open squares). Linear fits are shown for both untreated (solid line) and tirapazamine-treated conditions. (B) HL-60 cells (10^6 cells/ml) were incubated without drug (open circles) or with 50 μM tirapazamine (filled squares), 100 μM tirapazamine (filled triangles), 200 μM tirapazamine (filled diamonds), 500 μM tirapazamine (filled circles), or 1.0 mM tirapazamine (open squares). Linear fits for untreated and quadratic fits for tirapazamine-treated cells are shown as indicated. For treated cells, the point at $t = 0$ was added. (C) Values of calculated I are plotted versus tirapazamine concentration (filled squares). Values of I are also fitted to Eq. (4) using least-squares error (solid line).

profiles for untreated cells (open circles) and for cells treated with 50 μM tirapazamine (filled squares), 100 μM tirapazamine (filled triangles), 200 μM tirapazamine (filled diamonds), 500 μM tirapazamine (filled circles), or 1 mM tirapazamine (open squares). Results for untreated cells were fitted to a line ($r^2 = 0.996$) with a slope of $-0.637 \mu\text{M}/\text{min}$ (dashed line shown in Fig. 4B). Results for treated cells, which showed obvious curvature, were fitted to quadratics ($r^2 = 0.992, 0.986, 0.973, 0.975, \text{ and } 0.934$ for 50, 100, 200, 500, and 1000 μM tirapazamine, respectively). To the results for each condition was added one point, $[\text{O}_2]_0 = 225 \mu\text{M}$, which

assumes that all solutions were initially saturated with air at 37 $^\circ\text{C}$. Then results for untreated cells were fitted to a line $[\text{O}_2] = 187.5 \mu\text{M} - (0.713 \mu\text{M}/\text{min})t$ ($r^2 = 0.949$). Because of the low value of r^2 , results for untreated cells were fitted to a quadratic as with results for treated cells. The values of r^2 were then 0.974 for no tirapazamine and 0.991, 0.987, 0.981, 0.971, and 0.951 for 50, 100, 200, 500, and 1000 μM tirapazamine, respectively.

Values of $\langle k \rangle$ were calculated according to Eq. (3) with $d = 0$ and $t_f - t_i = 60$ min. The results are shown in Table 3, which gives $\langle k \rangle$ only for $t_i = 90$ and 150 min. Because all O_2 consumption profiles were fitted to quadratic forms, $\langle k \rangle$ is a linear function of t_i . For the calculation of $\langle k \rangle / \langle k \rangle_0$, the value of $\langle k \rangle_0$ is taken from this set of runs, not the previous set. The inhibitions of cellular respiration I at 90 min incubation were 10.5, 16.9, 7.4, 19.6, and 37.3% for treatment with 50, 100, 200, 500, and 1000 μM tirapazamine, respectively. (Results for 90 min are used here because 90 min is in the middle of the range of data being fitted.) As shown in Fig. 4C, these data were fitted to Eq. (5); the best fit had $I_{\text{max}} = 0.61$ and $A = 751 \mu\text{M}$ ($r^2 = 0.760$). Assuming that $I_{\text{max}} = 1$ (i.e., 100% inhibition) led to a much worse fit with $A = 1696 \mu\text{M}$ ($r^2 = 0.749$).

CsA

To investigate the effect of CsA on mitochondrial O_2 consumption, we incubated Jurkat cells (10^6 cells/ml) with CsA and measured oxygen concentrations alternately on five conditions. As shown in Fig. 5A, the five conditions were as follows: without drug (open circles) and with 20 nM CsA (filled triangles), 50 nM CsA (filled diamonds), 200 nM CsA (filled circles), or 500 nM CsA (filled squares). Because there was no evident curvature in these plots, all O_2 consumption profiles were fitted to linear functions. Thus, for $[\text{CsA}] = 0, 20, 50, 200, \text{ and } 500$ nM, linear fits ($r^2 = 0.989, 0.985,$

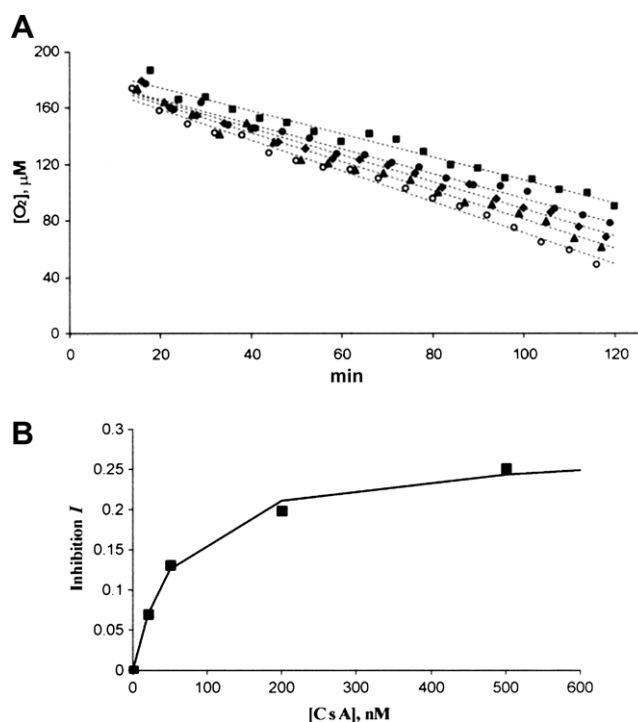


Fig. 5. Effects of CsA on cellular respiration. (A) Jurkat cells (10^6 cells/ml) were suspended in medium, 2 μM Pd phosphor, and 0.5% bovine serum albumin and were incubated without drug (open circles) or with 10 nM CsA (filled triangles), 50 nM CsA (filled diamonds), 200 nM CsA (filled circles), or 500 nM CsA (filled squares). Linear fits to the respiration profiles are shown as dashed lines. (B) Values of calculated inhibition I are plotted versus CsA concentration (filled squares). Values of I are also fitted to a function of least-squares error (solid line).

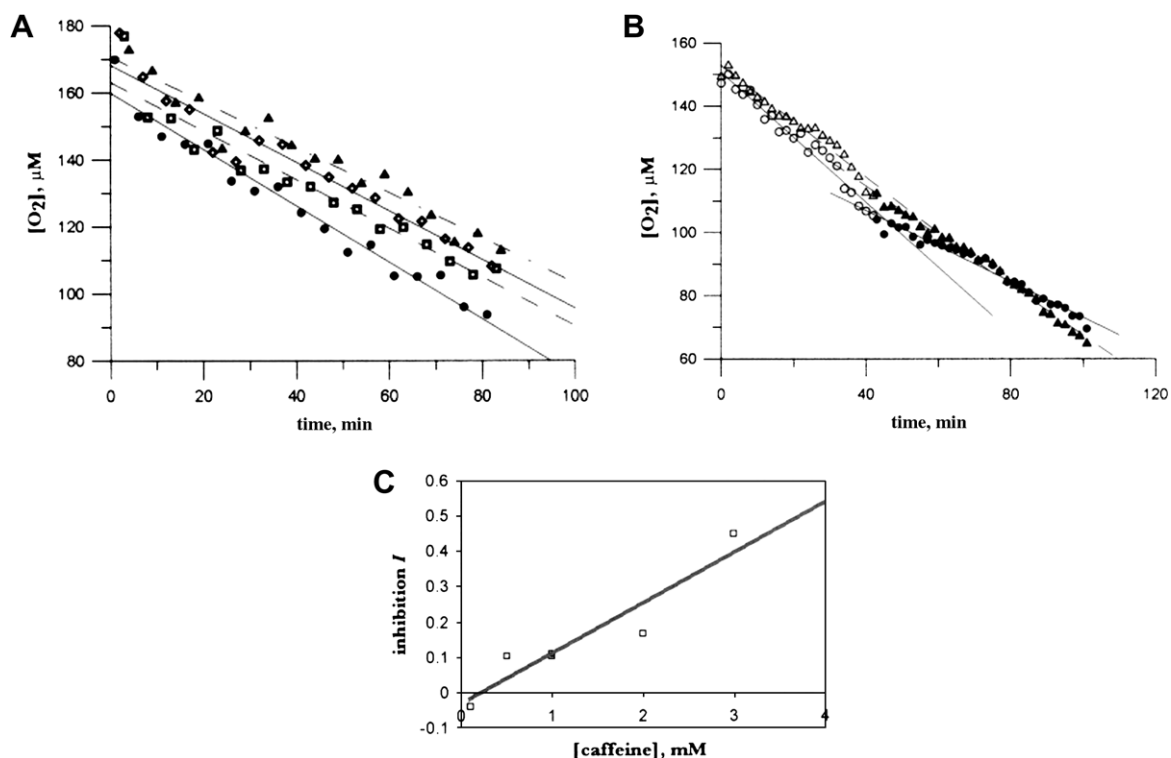


Fig. 6. Effects of caffeine on cellular respiration. HL-60 cells (10^6 cells/ml) were suspended in medium, $2 \mu\text{M}$ Pd phosphor, and 0.5% bovine serum albumin and were incubated in the presence or absence of caffeine. (A) Caffeine concentrations were 0.1 mM (filled circles), 0.5 mM (open diamonds), 1.0 mM (open squares), and 2.0 mM (filled triangles). Best linear fits are shown for all four conditions. (B) Oxygen concentrations were measured for approximately 40 min with no caffeine present, at which point caffeine was injected. Results of two separate experiments are shown, with least-squares fits before and after caffeine injection. In the first experiment (open and filled triangles with dashed line for fits), caffeine concentration was 2.0 mM. In the second experiment (open and filled circles with solid line for fits), caffeine concentration was 3.0 mM. (C) Inhibition $I = 1 - k/k_0$ calculated from respiration rates derived from experiments in panels A and B. Shown is best-fit straight line for I versus caffeine concentration.

0.984, 0.984, and 0.975, respectively) gave $\langle k \rangle = k = 1.10, 1.03, 0.99, 0.89,$ and $0.83 \mu\text{M O}_2/\text{min}$, respectively. (By putting $225 \mu\text{M}$ as the initial oxygen concentration $[\text{O}_2]_0$ and adopting quadratic fitting, r^2 values became worse (0.950, 0.969, 0.967, 0.965, and 0.966, respectively). It is clear from these results that the inhibitory effect of CsA on cellular respiration was dose dependent.

From the k values obtained from the linear fitting, we calculated $I = 1 - k/k_0$. Results are shown in Fig. 5B, with the best fit to Eq. (5) shown as a solid line and with $I_{\text{max}} = 0.272$ and $A = 57.9 \text{ nM}$ ($r^2 = 0.994$). When $I_{\text{max}} = 1$ (i.e., 100% inhibition) was assumed, the best value of A turned out to be 1150.3 nM , but $r^2 = 0.598$, so this fitting cannot be adopted.

Caffeine

We investigated the effect of pure caffeine (powder formulation without vehicle) on HL-60 cellular respiration. The cells (10^6 cells/ml) were suspended in medium plus $2 \mu\text{M}$ Pd phosphor and 0.5% albumin with the addition of 0.1, 0.5, 1.0, or 2.0 mM caffeine. Caffeine was dissolved in the medium and added to the cell suspension immediately prior to O_2 measurement. Measurements were made alternately on the four samples. Results are shown in Fig. 6A. Here k values were obtained from the slopes of the best linear fits because going to quadratic fits produced no improvement. For the four concentrations of caffeine, we found $k = 0.843, 0.726, 0.727,$ and $0.676 \mu\text{M O}_2/\text{min}$ ($r^2 = 0.966, 0.941, 0.929,$ and 0.946 , respectively). From the four k values, linear extrapolation to 0 concentration produced $k_0 = 0.8090 \pm 0.0364$. This value of k_0 was used to calculate the inhibitions for the four concentrations, which were $-0.042, 0.102, 0.101,$ and 0.165 , respectively.

Fig. 6B shows results of two separate experiments to test whether the effect of caffeine on HL-60 respiration was immedi-

ate. After O_2 measurement proceeded for approximately 40 min, caffeine was injected into the vials and O_2 measurement was continued. The results for 1 mM caffeine are shown by empty and filled triangles in Fig. 2B, with best-fit lines (before and after caffeine addition) shown as dashed. The k value before addition was $0.883 \mu\text{M O}_2/\text{min}$ and was reduced instantly to $0.787 \mu\text{M O}_2/\text{min}$ after addition (11% inhibition). For 3.0 mM caffeine (data not shown), the k value before addition was $1.028 \mu\text{M O}_2/\text{min}$ and was reduced instantly to $0.568 \mu\text{M O}_2/\text{min}$ after addition (45% inhibition).

All of the inhibitions from the experiments of Figs. 6A and 6B are plotted versus caffeine concentration in Fig. 6C. Here $I = 1 - k/k_0$. The best-fit line is also shown; it comes very close to passing through (0,0) as expected. There is no sign of saturation (i.e., leveling off in the plot of I vs. [caffeine]) in this range of concentrations, so no attempt was made to fit to Eq. (5).

Discussion

The use of respiratory monitoring is proposed here to assess the extent of drug-impaired cellular function and how it depends on parameters such as incubation time and dosage. To obtain respiration rates, we measure $[\text{O}_2]$ using phosphorescence decay (other methods could also be used [26,27]). Although different drugs attack different cellular targets such as mitochondria, DNA, and thiols, their inhibitory effects on the mitochondrial function sometimes appear to be similar. Clearly, answering the question of why a particular drug gives a specific cellular respiration pattern requires more understanding of the drug-cell interaction than is currently available. However, differences in oxygen consumption profiles (Figs. 1–6) indicate different mechanisms of action for dif-

ferent drugs. The diverse profiles make it important to characterize the drug effect by a single parameter such as the inhibition I .

To measure the extent of inhibition of mitochondrial oxygen consumption, various cell lines were exposed continuously to a variety of cytotoxic drugs. For testing, the cells and the cytotoxic compounds were sealed in a closed vessel that also contained growth medium, sufficient glucose (as a respiratory substrate), and the Pd phosphor. Untreated cells consume O_2 at a constant rate, whereas drug-treated cells exhibit a diversity of O_2 consumption profiles (linear or nonlinear).

Oxygen concentration is fit to a linear (Pt compounds and CsA) or quadratic (dactinomycin, doxorubicin, and tirapazamine) function of time. Fitting to a higher order, such as cubic or polynomial, can be applied on the condition that the fit is significantly improved (i.e., r^2 significantly increased). The rate of respiration k is the negative of the slope of a plot of $[O_2]$ versus time as calculated from the fitting function. The time average respiration rate is proposed as a characteristic parameter. It is obtained by integrating k over a well-defined time interval. Then the inhibition I is calculated as $1 - \langle k \rangle / \langle k \rangle_0$, where $\langle k \rangle_0$ is the average value of k for cells not treated by drug. It is important to obtain $\langle k \rangle$ and $\langle k \rangle_0$ from measurements on the same batch of cells. For the most meaningful comparison, the measurements of $[O_2]$ should be done simultaneously (i.e. alternately) on treated and untreated cells.

When I has been measured for a series of drug concentrations D , it is convenient to fit the results to the two-parameter function, $I = I_{\max} D / (D + A)$. The value of I provides a simple and convenient characterization of drug cytotoxicity. (Other measures of drug cytotoxicity continue to be suggested [28–30].) It also helps to predict the dosing necessary to shut down respiration of malignant cells and, thus, may be useful in assessing the efficiency of anticancer drugs.

Acknowledgment

This work was supported by a fund from the Paige's Butterfly Run.

References

- [1] J.E. Ricci, R.A. Gottlieb, D.R. Green, Caspase-mediated loss of mitochondrial function and generation of reactive oxygen species during apoptosis, *J. Cell Biol.* 160 (2003) 65–75.
- [2] J.E. Ricci, C. Munoz-Pinedo, P. Fitzgerald, B. Bailly-Maitre, G.A. Perkins, N. Yadava, I.E. Scheffer, M.H. Ellisman, D.R. Green, Disruption of mitochondrial function during apoptosis is mediated by caspase cleavage of the p75 subunit of complex I of the electron transport chain, *Cell* 117 (2004) 773–786.
- [3] K.M. Debatin, Apoptosis pathways in cancer and cancer therapy, *Cancer Immunol. Immunother.* 53 (2004) 153–159.
- [4] S.W. Lowe, H.E. Ruley, T. Jacks, D.E. Housman, p53-Dependent apoptosis modulates the cytotoxicity of anticancer agents, *Cell* 74 (1993) 954–967.
- [5] F. Zunino, G. Capranico, DNA topoisomerase II as the primary target of anti-tumor anthracyclines, *Anticancer Drug Des.* 5 (1990) 307–317.
- [6] J.H. Doroshow, K.J. Davis, Redox cycling of anthracyclines by cardiac mitochondria: II. Formation of superoxide anion, hydrogen peroxide, and hydroxyl radical, *J. Biol. Chem.* 261 (1986) 3068–3074.
- [7] W. Muller, D.M. Crother, Studies of the binding of actinomycin and related compounds to DNA, *J. Mol. Biol.* 35 (1968) 251–290.
- [8] J. Goodisman, D. Hagrman, K.A. Tacka, A.K. Souid, Analysis of cytotoxicities of platinum compounds, *Cancer Chemother. Pharmacol.* 57 (2006) 257–267.
- [9] J.M. Brown, SR 4233 (tirapazamine): A new anticancer drug exploiting hypoxia in solid tumors, *Br. J. Cancer* 67 (1993) 1163–1170.
- [10] J.S. Daniels, K.S. Gates, DNA cleavage by the antitumor agent 3-amino-1,2,4-benzotriazine-1,4-dioxide (SR4233): Evidence for involvement of hydroxyl radical, *J. Am. Chem. Soc.* 118 (1996) 3380–3385.
- [11] J. Wang, K.A. Biedermann, J.M. Brown, Repair of DNA and chromosome breaks in cells exposed to SR 4233 under hypoxia or to ionizing radiation, *Cancer Res.* 52 (1992) 4473–4477.
- [12] M.M. Merker, R.E. Handschumacher, Uptake and nature of the intracellular binding of cyclosporin A in a murine thymoma cell line, BW5147, *J. Immunol.* 132 (1984) 3064–3070.
- [13] P.M. Colombani, A. Robb, A.D. Hess, Cyclosporin A binding to calmodulin: A possible site of action on T lymphocytes, *Science* 228 (1985) 337–339.
- [14] K.M. Broekemeier, M.E. Dempsey, D.R. Pfeiffer, Cyclosporin A is a potent inhibitor of the inner membrane permeability transition in liver mitochondria, *J. Biol. Chem.* 264 (1989) 7826–7830.
- [15] V. Petronilli, C. Cola, S. Massari, R. Colonna, P. Bernardi, Physiological effectors modify voltage sensing by the cyclosporin A-sensitive permeability transition pore of mitochondria, *J. Biol. Chem.* 268 (1993) 21939–21945.
- [16] N. Fournier, G. Ducet, A. Crevat, Action of cyclosporine on mitochondrial calcium fluxes, *J. Bioenerg. Biomembr.* 19 (1987) 297–303.
- [17] J.M. Vanderkooi, D.F. Wilson, A new method for measuring oxygen concentration in biological systems, *Adv. Exp. Med. Biol.* 200 (1986) 189–193.
- [18] W.L. Rumsey, J.M. Vanderkooi, D.F. Wilson, Imaging of phosphorescence: A novel method for measuring oxygen distribution in perfused tissue, *Science* 241 (1988) 1649–1651.
- [19] D.F. Wilson, Oxygen dependent quenching of phosphorescence: A perspective, *Adv. Exp. Med. Biol.* 317 (1992) 195–201.
- [20] M. Pawlowski, D.F. Wilson, Monitoring of the oxygen pressure in the blood of live animals using the oxygen dependent quenching of phosphorescence, *Adv. Exp. Med. Biol.* 316 (1992) 179–185.
- [21] Z. Tao, H.G. Withers, H.S. Penefsky, J. Goodisman, A.K. Souid, Inhibition of cellular respiration by doxorubicin, *Chem. Res. Toxicol.* 19 (2006) 1051–1058.
- [22] Z. Tao, S.S. Ahmad, H.S. Penefsky, J. Goodisman, A.K. Souid, Dactinomycin impairs cellular respiration and reduces accompanying ATP formation, *Mol. Pharm.* 3 (2006) 762–772.
- [23] Z. Tao, H.S. Penefsky, J. Goodisman, A.K. Souid, Caspase activation by anticancer drugs: The caspase storm, *Mol. Pharm.* 4 (2007) 583–595.
- [24] Z. Tao, M.P. Morrow, H.S. Penefsky, J. Goodisman, A.K. Souid, Study on caspase-induced mitochondrial dysfunction by anticancer drugs, *Curr. Drug Ther.* 2 (2007) 233–235.
- [25] Z. Tao, J. Goodisman, A.K. Souid, Oxygen measurement via phosphorescence: Reaction of sodium dithionite with dissolved oxygen, *J. Phys. Chem. A* 112 (2008) 1511–1518.
- [26] L.A.M. Pouvreau, M.J.F. Strampraad, S. Van Berloo, J.H. Kattenberg, S. deVries, NO, N₂ O, and O₂ reaction kinetics: Scope and limitations of the Clark electrode, *Methods Enzymol.* 436 (2008) 97–112.
- [27] J. Jiang, L. Gao, W. Zhong, S. Meng, B. Yong, Y. Song, X. Wang, C. Bai, Development of fiber optic fluorescence oxygen sensor in both in vitro and in vivo systems, *Respir. Physiol. Neurobiol.* 161 (2008) 160–166.
- [28] R. Mirzayana, B. Andrais, A. Scott, A. Tessier, D. Murray, A sensitive assay for the evaluation of cytotoxicity and its pharmacologic modulation in human solid tumor-derived cell lines exposed to cancer-therapeutic agents, *Can. J. Pharmacy Pharm. Sci.* 10 (2007) 298S–311S.
- [29] Y. Zhong, A.C. Bakke, G. Fan, R.M. Braziel, K.M. Gatter, J.F. Leis, R.T. Maziarz, J.Z. Huang, Drug resistance in B-cell chronic lymphocytic leukemia: Predictable by in vitro evaluation with a multiparameter flow cytometric cytotoxicity assay, *Cytometry B Clin. Cytom.* 72 (2007) 189–195.
- [30] W. Li, M.S. Lam, A. Birkeland, A. Riffel, L. Montana, M.E. Sullivan, J.M. Post, Cell-based assays for profiling activity and safety properties of cancer drugs, *J. Pharmacol. Toxicol. Methods* 54 (2006) 313–319.